Journal of Magnetism and Magnetic Materials 454 (2018) 139–143

Contents lists available at ScienceDirect

Journal of Magnetism and Magnetic Materials

journal homepage: www.elsevier.com/locate/jmmm

Research articles

Weak ferromagnetism along the third-order axis of the $FeBO_3$ crystals caused by Fe^{2+} impurity ions

S.G. Ovchinnikov, V.V. Rudenko *, A.M. Vorotynov

Kirensky Institute of Physics, Federal Research Center KSC SB RAS, Akademgorodok 50, bld. 38, Krasnoyarsk 660036 Russia

ARTICLE INFO

Article history:
Received 10 December 2017
Accepted 15 January 2018
Available online 31 January 2018

Keywords:
Week ferromagnetism
Magnetic anisotropy
Impurity

ABSTRACT

Using the single-ion approximation, the weak ferromagnetic moment $\sigma_Z(Fe^{2+})$ along the third-order axis of $FeBO_3$ crystals, which is caused by the contribution of Fe^{2+} ions, has been investigated in the framework of the model Fe^{2+} impurity ion –BO_3 vacancy. The extreme low-temperature behavior of the total magnetic moment due to the strong dependence of the Fe^{2+}ion contribution is predicted.

© 2018 Published by Elsevier B.V.

1. Introduction

Iron borate crystals were synthesized fairly long ago and have been well-studied, but still attract close attention of researches as suitable objects for the development of various magnetism-related models. These crystals have a relatively simple lattice, high Neel temperature, narrow antiferromagnetic resonance lines, and a series of isostructural diamagnetic analogs. In particular, in 2014, Dmitrienko et al. [1] determined first the sign and value of the vector components in the Dzyaloshinskii–Moriya interaction using iron borate crystals. Kalashnikova et al. [2] lately observed the effect of pulse excitation of interacting magnetic moments by the linearly polarized light in $FeBO_3$. In addition, using the isostructural diamagnetic analogs with the trivalent iron impurity and the electron spin resonance technique (ESR), the uniaxial magnetic anisotropy (the c_3 third-order axis in the basal plane) in magneto-concentrated crystals with ions in the S state was quantitatively described [3]. In contrast to the uniaxial anisotropy [3], the magnetic system of the crystal, despite its simple crystal lattice (calcite structure), exhibits a relatively complex behavior upon rotation of the antiferromagnetism vector $\boldsymbol{l} = (\boldsymbol{M}_1 - \boldsymbol{M}_2)/M$ in the (1 1 1) plane [4,5]. Such a complex behavior is typical, in particular, of the ferromagnetism vector $\boldsymbol{m} = (\boldsymbol{M}_1 + \boldsymbol{M}_2)/M$ $(M = 2|\boldsymbol{M}_1| = 2|\boldsymbol{M}_2|)$ with regard to the last term in free energy (1) written by Dzyaloshinskii:

$$\Phi = (1/2)Bm^2 + (1/2)a\cos^2\theta + (1/2)c\cos^4\theta + d\sin\theta(m_y\cos\phi - m_x\sin\phi) + q\sin^3\theta\cos\theta\cos 3\phi + tm_z\sin^3\theta\sin 3\phi \quad (1)$$

Here, the first term characterizes the isotropic exchange energy of the crystal; the second and third terms, the uniaxial anisotropy; the fourth term, the Dzyaloshinskii interaction leading to the onset of weak ferromagnetism in the (1 1 1) basal plane; the last two terms, the anisotropy energy in the (1 1 1) plane; θ and φ are the polar and azimuthal angles of the vector $\boldsymbol{l}$, which are counted from the third-order (z) axis and from the crystal symmetry plane (x axis), respectively. Note that the weak ferromagnetism of the crystals was thoroughly investigated by Turov [5].

The phenomenological expression for the relative weak ferromagnetic moment along the c_3 axis is obtained by minimizing free energy (1) with respect to m_z:

$$m_z = (-t/B)\sin^3\theta\sin 3\varphi. \quad (2)$$

The measured weak ferromagnetic moment along the c_3 axis has the form $\sigma_z(T) = m_z M$ [6]. However, as was observed in different experiments [7,8], the basal anisotropy caused by the next-to-last term in Eq. (1) changes from one sample to another and contains the uniaxial component [7] in the (1 1 1) plane of the $FeBO_3$ crystals.

2. Impurity anisotropy. Phenomenological description

In this work, we discuss the weak ferromagnetic moment along the third-order axis in the framework of the model BO_3 vacancy – Fe^{2+} ion. The BO_3^{3-} ions are tightly covalently bound and can exist

* Corresponding author at: Kirensky Institute of Physics SB RAS, Akademgorodok 50, bld. 38, Krasnoyarsk 660036 Russia.
E-mail addresses: sgo@iph.krasn.ru (S.G. Ovchinnikov), rvv@iph.krasn.ru (V.V. Rudenko).

https://doi.org/10.1016/j.jmmm.2018.01.037
0304-8853/© 2018 Published by Elsevier B.V.

in the melt–solution at the crystal growth temperatures as a whole. The ions are spatially extended and therefore hardly incorporate into a growing crystal. As a result, vacancies of these groups and, consequently, the Fe^{2+} impurity, occur. A part of these vacancies will apparently be compensated by divalent lead ions, the oxide and fluoride of which was used as solvents during the $FeBO_3$ crystal growth [9]. The relative concentration of the BO_3 vacancies is $\ll 1$. A vacancy is surrounded by six nearest iron ions, one of which is Fe^{2+} (Figs. 1 and 2).

Upon rotation of the external field in the basal plane (in the experiment) or in the case when the effective basal anisotropy becomes equal to the potential barrier under the action of temperature, the electron motion around the BO_3 vacancy will be observed.

Figs. 1 and 2 show the distribution of crystal field axes by means of the BO_3 vacancy on the Fe^{2+} iron ions. Dashed and solid arrows have the negative and positive components on the Z axis, respectively. The Z axis is perpendicular to the figure plane. In the figure, Z_H coordinates of borate groups and iron ions along the third-order axis in the hexagonal setting are presented. The X axis lies in the crystal symmetry plane.

The analogous axes distribution follows from the ESR data for the Fe^{3+} and Mn^{2+} ions surrounded by the BO_3^{3-} ions and by the CO_3^{2-} ions in MBO_3 (M = Ga, Sc,) [10] and isostructural $CaCO_3$ [11]. In the model used, we will take into account the magnetic anisotropy of the Fe^{2+} ions, while the Fe^{3+}contribution will be ignored. The iron ions in positions 1 and 2 are assumed to be antiferromagnetically ordered. The point local symmetry of the Fe^{2+} ion positions is c_1 and the basal anisotropy is therefore described by the triclinic symmetry tensor. The anisotropy energy in the $X'Y'Z'$ moving coordinate system located on ions in positions 1 and 2 is $E_k = \sum_{nl} B_{knl} M_{kn} M_{kl}$. Here, k can take the values from 1 to 3 (complex 1) and from 1′ to 3′ (complex 2) for all iron ions involved in redistribution of Fe^{2+} and surrounding the BO_3 vacancies in positions 1 and 2 (Figs. 1 and 2); $n, l = X', Y', Z' \rightarrow 1, 2, 3$ and $1', 2', 3'$; M_{kn}, M_{kl} are the projections of a unit sublattice magnetic moment k of the ion onto the corresponding $X'Y'Z'$ system axes; and B_{knl} is the tensor of the basal anisotropy of triclinic symmetry in the $X'Y'Z'$ coordinate system of the k ion. We write the anisotropy energy in the unified coordinate system. We transform B_{knl} at the rotation of the $X'Y'Z'$ coordinate system [12] around the third-order axis c_3 by angles $\alpha + \beta$ and $\alpha - \beta$ (here, α introduced instead of k takes values of $0, -120, -240°$). The counterclockwise rotation direction is assumed to be positive. During rotation, the X' axis coinciding with the projection of solid axes 1, 2, 3 (Fig. 1) and dashed axes $1', 2', 3'$ (Fig. 2) onto the (1 1 1) plane lied in the X axis; thus, taking into account that in the description of the experiment the anisotropy tensor should have a symmetry center, we obtain in the polar system of coordinates for one ion

$$\begin{aligned} E_{i\alpha} &= (1/2)(B_{11} + B_{22}) + [B_{33} - (1/2)(B_{11} + B_{22})] \cos^2 \theta_i' \\ &+ (1/2)(B_{11} - B_{22}) \cos 2(\varphi_i' + \alpha + \beta_i) \sin^2 \theta_i' \\ &+ B_{12} \sin 2(\varphi_i' + \alpha + \beta_i) \sin^2 \theta_i' + B_{13} \cos(\varphi_i' + \alpha + \beta_i) \sin 2\theta_i' \\ &+ B_{23} \sin(\varphi_i + \alpha + \beta_i) \sin 2\theta_i', \end{aligned} \quad (3)$$

for Fe^{2+} in the first position $(+\beta, i = 1)$ (Fig. 1) and for Fe^{2+} in the second position $(-\beta, i = 2)$ (Fig. 2). Here, θ_1', θ_2' and φ_1', φ_2' are the polar and azimuthal angles for the sublattice magnetic moments of the Fe^{2+} ions, respectively. When writing Eq. (3), we took into account the correlation between the constants in accordance with [13]. Introducing the angles $\varphi_1' = \varphi'$, $\varphi_2' = \varphi' + \pi$, and a part of angles $\theta_1' = \theta', \theta_2' = \pi - \theta$ for the antiferromagnetism vector so that the terms at $\cos\theta_1' + \cos\theta_2'$ and expressions with the angular variables $2(\varphi' + \alpha)$ were kept, we obtain from (3) for one ion

$$\begin{aligned} E_\alpha &= (1/2)(B_{11} + B_{22}) + [B_{33} - (1/2)(B_{11} + B_{22})] \cos^2 \theta' \\ &+ (1/2)(B_{11} - B_{22}) \cos 2\beta \cos 2(\varphi' + \alpha) \sin^2 \theta' + B_{12} \\ &\times \cos 2\beta \sin 2(\varphi' + \alpha) \sin^2 \theta' - B_{13} \sin \beta (\cos\theta_1' + \cos\theta_2') \\ &\times \sin(\varphi' + \alpha) \sin\theta' + B_{23} \sin\beta (\cos\theta_1' + \cos\theta_2') \cos(\varphi' \\ &+ \alpha) \sin\theta' \end{aligned} \quad (4)$$

with regard to

$$\sin^2\theta_1' + \sin^2\theta_2' \cong 2\sin^2\theta', \sin^2\theta_1' - \sin^2\theta_2' \cong 0$$
$$\sin 2\theta_1' - \sin 2\theta_2' \cong \sin 2\theta', \sin 2\theta_1' + \sin 2\theta_2' \cong 2\sin\theta'(\cos\theta_1' + \cos\theta_2').$$

Note that, in Eq. (4), the account for the expressions with the arguments $2(\varphi' + \alpha)$, which intersect with the term at $(\cos\theta_1' + \cos\theta_2')$ due to the quadratic contribution in (5) (see

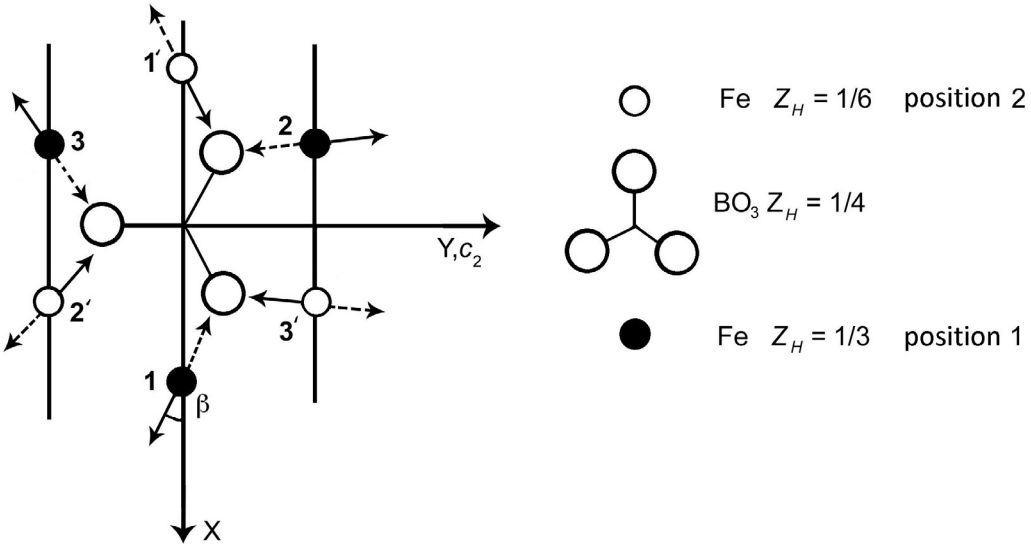

Fig. 1. Distribution of the crystal field axes on Fe^{2+} ions by means of the BO_3 vacancy of the BO_3^{3-} ion (complex 1).

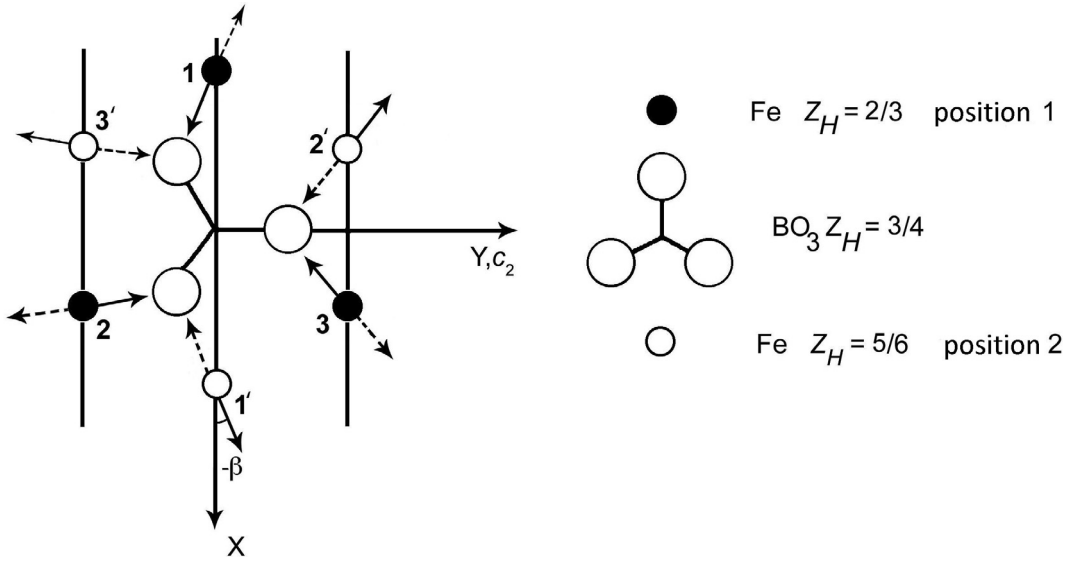

Fig. 2. Distribution of the crystal field axes on Fe^{2+} ions by means of the BO_3 vacancy of the BO_3^{3-} ion (complex 2).

below), leads to the formation of the angular dependence of the basal anisotropy energy caused by the weak ferromagnetic moment along the third-order axis $m'_z(Fe^{2+})$.

We designate the divalent iron ions lying in the directions $\alpha = 0, -120, -240^\circ$ as $\alpha \to n \to$ 1, 2, 3 for the first sublattice (Fig. 1) and $1', 2'3'$ for the second sublattice (Fig. 2) and determine the relative concentration n in the c_n direction from the kinetic equations, as was made in [14]. We will consider electron hoppings between ions $1-2-3$ (Fig. 1) and $1'-2'-3'$ (Fig. 2) in accordance with the symmetry of the BO_3^{3-} vacancies. In this case, the electron hoppings will be correlated (due to the long-range order) by the simultaneous motion, e.g., in positions $1 \to 2$ (Fig. 1) and $1' \to 2'$ (Fig. 2). In the experiment, in the applied magnetic field with a certain value rotating in the basal crystal plane, the electron will move around the vacancies in complexes1 and 2. At certain values of the external magnetic field rotating in the basal plane, temperature, and crystal complex parameters, both the hexagonal and uniaxial anisotropies will be observed. The uniaxial anisotropy occurs due to the electron hopping freezing at low temperatures.

We denote the potential barrier overcome by electrons during their hoppings by E_b and the anisotropy energy for each direction in the crystal lattice, by $E_n (n = 1, 2, 3)$. Then, the rate of variation in the Fe^{2+} concentration $\dot{c}_n$, e.g., in direction 1, will be proportional to the electron hopping frequency, Boltzmann factor, and c_n in the corresponding positions:

$$\dot{c}_1 = -2v_0c_1\exp[-(E_b - E_1)/kT] + v_0c_2\exp[-(E_b - E_2)/kT] + v_0c_3 \times \exp[-(E_b - E_3)/kT],$$

where v_0 is the frequency of electron hoppings between positions at $kT \gg |E_b - E_n|$, k is the Boltzmann constant, T is the temperature, and c_3 is the concentration (in contrast to the designation of the third-order axis). The total system of linear differential equations will have the form

$$\begin{pmatrix} \dot{c}_1 \\ \dot{c}_2 \\ \dot{c}_3 \end{pmatrix} = v \begin{pmatrix} -2\exp(E_1/kT)\exp(E_2/kT)\exp(E_3/kT) \\ \exp(E_1/kT) - 2\exp(E_2/kT)\exp(E_3/kT) \\ \exp(E_1/kT)\exp(E_2/kT) - 2\exp(E_3/kT) \end{pmatrix} \begin{pmatrix} c_1 \\ c_2 \\ c_3 \end{pmatrix}$$

Here, $v = v_0\exp(-E_b/kT)$.

Solving the system of linear differential equations using a standard technique from [15], obtain

$$c_1 = B_1 + B_2\exp(pvt') + B_3\exp(rvt')$$

$$c_2 = \frac{A_1B_1}{A_2} + \frac{3A_1 + p}{3A_2 + p}B_2\exp(pvt') + \frac{3A_1 + r}{3A_2 + r}B_3\exp(rvt'),$$

$$c_3 = \frac{A_1B_1}{A_3} + \frac{3A_1 + p}{3A_3 + p}B_2\exp(pvt') + \frac{3A_1 + r}{3A_3 + r}B_3\exp(rvt'),$$

where $A_n = \exp(E_n/kT)$,

$$p = -(A_1 + A_2 + A_3) + \sqrt{A_1^2 + A_2^2 + A_3^2 - (A_1A_2 + A_1A_3 + A_2A_3)},$$

$$r = -(A_1 + A_2 + A_3) - \sqrt{A_1^2 + A_2^2 + A_3^2 - (A_1A_2 + A_1A_3 + A_2A_3)},$$

B_1, B_2, B_3 are the constants determined from the limit conditions, and t' is the time parameter.

Let us consider the equilibrium state ($t = \infty$). Then,

$$B_1 = c_1^0 = (1/A_1)/\sum_n(1/A_n), c_n^0 = (1/A_n)/\sum_n(1/A_n).$$

The impurity anisotropy energy per mole of the $FeBO_3$ crystal substance can be presented accurate to the quadratic expansion term as

$$E = Nc_0\sum_{n=1}^{3}c_n^0E_n \simeq (Nc_0/3)\left[\sum_n E_n - (1/kT)\sum_n E_n^2\right]. \quad (5)$$

Here, $c_0 = (N'/N)$, N is the Avogadro number, N' is the number of Fe^{2+} ions in one mole of $FeBO_3$, and c_n^0 is the relative equilibrium concentration of Fe^{2+} ions in direction n. Energy (5) can be rewritten after regrouping the expansion terms in the form

$$E = -Nc_0[2B_{12}B_{23} - B_{13}(B_{11} - B_{22})](1/kT)\sin\beta\cos 2\beta m'_z(Fe^{2+}) \times \sin^3\theta'\sin 3\varphi' - Nc_0[2B_{12}B_{13} + B_{23}(B_{11} - B_{22})](1/kT) \times \sin\beta\cos 2\beta m'_z(Fe^{2+})\sin^3\theta'\cos 3\varphi' + Nc_0[B_{33} - (1/2)(B_{11} + B_{22})]\cos^2\theta',$$

Here, according to the definition, $\cos\theta'_1 + \cos\theta'_2 = 2m'_z(Fe^{2+})$.

We present the free energy Φ' in form (6), where we introduce the isotropic exchange term, phase angle ψ, and constant $A = -[2B_{12}B_{23} - B_{13}(B_{11} - B_{22})]$, $D = -[2B_{12}B_{13} + B_{23}(B_{11} - B_{22})]$.

$$\Phi' = (1/2)B'\boldsymbol{m}'^2(Fe^{2+}) + Nc_0[B_{33} - (1/2)(B_{11} + B_{22})]\cos^2\theta'$$
$$+ Nc_0[A\sin 3\varphi' + D\cos 3\varphi']\cos 2\beta \sin\beta m'_z(Fe^{2+})[1/kT]\sin^3\theta'$$
$$= (1/2)B'\boldsymbol{m}'^2(Fe^{2+}) + Nc_0[B_{33} - (1/2)(B_{11} + B_{22})]\cos^2\theta'$$
$$+ Nc_0\sqrt{A^2 + D^2}\sin\beta\cos 2\beta m'_z(Fe^{2+})[1/kT]\sin^3\theta'$$
$$\times\cos(3\varphi' - \psi')B'\ Fe^{2+},\ Fe^{2+} - Fe^{3+} - Fe^{2+}, \cos(3\varphi' - \psi')$$
$$= \cos 3\varphi'\cos\psi' + \sin 3\varphi'\sin\psi'$$
$$= (\cos 3\varphi')(D/\sqrt{A^2 + D^2}) + \sin(3\varphi')(A/\sqrt{A^2 + D^2}), \quad (6)$$

$$\mathrm{tg}\psi' = (A/D) = \frac{2B_{12}B_{23} - B_{13}(B_{11} - B_{22})}{2B_{12}B_{13} + B_{23}(B_{11} - B_{22})}$$

Here, B' is the exchange constant of the Fe^{2+} impurity determined by the interaction Fe^{2+}– Fe^{3+}– Fe^{2+}. In the basal plane of the $FeBO_3$ crystal, there are two types of nonequivalent directions determined by the crystal symmetry: three symmetry planes and three second-order axes. Let $\psi' = 90^\circ$ in Eq. (6), which, in the long run, will be consistent with Eq. (2). The constant D is zero due to the crystal symmetry.

Minimizing (6) with respect to $m\prime_z(Fe^{2+})$, we find the relative weak ferromagnetic moment along the third-order axis of the $FeBO_3$ crystal:

$$m'_z(Fe^{2+}) = \pm|(Nc_0A/kTB')\sin\beta\cos 2\beta|\sin^3\theta'\sin 3\varphi' \quad (7)$$

In (7), the parentheses indicate the absolute value.

3. Impurity anisotropy. "Microscopic description

Let us consider the effect of Fe^{2+} impurity ions on the temperature dependence of the weak ferromagnetic moment along the third-order axis of the $FeBO_3$ crystals. According to [16], the Fe^{2+} ion can be in the singlet or doublet ground orbital state, depending on whether the axial electric field potential along the trigonal axis is minimum or maximum. Calculation of the coefficient $(1/2)B_2^0$ [17] in the expression for the potential [18] yields the positive sign. Therefore, the potential in its form presented in [16,18] will be minimum and, according to [16,18], the three lower energy levels can be described by the effective spin $s' = 1$.

The Hamiltonian for the Fe^{2+} impurity ion in the single-ion approximation in the case of the lowest symmetry has the form [19]

$$\mathcal{H} = g\mu_B\boldsymbol{H}_i^{eff}\boldsymbol{s}'_i + A_2^0O_{2i}^0 + A_2^1O_{2i}^1 + A_2^2O_{2i}^2 + \tilde{A}_2^1\tilde{O}_{2i}^1 + \tilde{A}_2^2\tilde{O}_{2i}^2,$$

where $i = 1$ and 2 correspond to the first and second positions. The first expression is the isotropic exchange energy in the molecular field approximation. Here, H_i^{eff} is the exchange field caused by the effect of the Fe^{3+} ions on the Fe^{2+} ion and $\boldsymbol{s}'_i$ is the spin of the Fe^{2+} ion. The operators O_j^l and $\tilde{O}_j^l$ were given, e.g., in [19]. The solution of the problem on the eigenvalues of this Hamiltonian yields the expression for energy levels obtained in the first order of the perturbation theory

$$E_{i\alpha m_i} = g\mu_BH_i^{eff}m_i + \left[\frac{A_2^0}{2}(3\cos^2\theta'_i - 1)\right.$$
$$+\frac{A_2^1}{4}\sin 2\theta'_i\cos(\varphi'_i + \alpha \pm \beta) + \frac{\tilde{A}_2^1}{4}\sin 2\theta'_i\sin(\varphi'_i + \alpha \pm \beta)$$
$$\left.+\frac{A_2^2}{2}\sin^2\theta'_i\cos 2(\varphi'_i + \alpha \pm \beta) + \frac{\tilde{A}_2^2}{2}\sin^2\theta'_i\sin 2(\varphi'_i + \alpha \pm \beta)\right]$$
$$\times(3m_i^2 - 2) \quad (8)$$

Here, α indicates the directions in the (1 1 1) plane and amounts to 0, (−)120, (−)240°, +β is the angle for the first position and −β is the angle for the second position, and μ_B is the Bohr magneton.

The temperature dependence of the phenomenological anisotropy constants follows from the comparison of Eqs. (3) and (8) with regard to the calculated free energy

$$F(Fe^{2+}) = -(Nc_0kT/2)\sum_i \ln Z_i; Z_i = \sum_{\alpha m'_i}\exp(-E_{i\alpha m'_i}/kT).$$

Here, m'_i is the magnetic quantum number of the ith ion, N is the Avogadro number, c_0 is the Fe^{2+} ion concentration in the crystal, T is the temperature, and k is the Boltzmann constant. The analogous calculation of F was described in detail in [6]. The phenomenological constants of the anisotropy tensor and their "microscopic" expressions (for one ion) are related as

$$B_{33} - (1/2)(B_{11} + B_{22}) = (3/2)A_2^0(z'_1/z'_0),$$
$$B_{13} = (1/4)A_2^1(z'_1/z'_0),$$
$$B_{23} = (1/4)\tilde{A}_2^1(z'_1/z'_0),$$
$$(1/2)(B_{11} - B_{22}) = (1/2)A_2^2(z'_1/z'_0),$$
$$B_{12} = (1/2)\tilde{A}_2^2(z'_1/z'_0),$$

where

$$(z'_1/z'_0) = (1 - Y')^2/(1 + Y' + Y'^2), Y'$$
$$= \exp[-g\mu_BH^{eff}(0)B_{5/2}(x)/kT], H^{eff}(0) = 3\cdot 10^6\mathrm{Oe}.$$

Using the results obtained, for the measured impurity weak ferromagnetic moment along the third-order axis per mole of the $FeBO_3$ crystal substance, we have

$$\sigma'_z(Fe^{2+}) = m'_z(Fe^{2+})M'(Fe^{2+})$$
$$= \pm\frac{Nc_0|A'_{imp}|}{kTH^{eff}(0)B_{5/2}(x)}\left(\frac{z'_1}{z'_0}\right)^2\sin^3\theta'\sin 3\varphi'.$$

Here, $M' = Nc_0g\mu_Bs'B_1(x)$, $s' = 1$, g is the spectroscopic splitting factor, $B_1(x)$ is the Brillouin function for the spin equal to 1, $|A'_{imp}|$ is the absolute value of the constant including the constants of energy levels (8) per one ion with the squared energy dimensionality, and k is the Boltzmann constant. Since in the experiment the weak ferromagnetic moment along the c_3 axis is measured in the fields much stronger than the basal anisotropy, we can use the unified coordinates in $\sigma_z(T)$, including the contributions of the Fe^{2+} and Fe^{3+} ions [6].

4. Discussion of the results

Fig. 3 shows the calculated temperature dependence proportional to the weak ferromagnetic moment along the third-order axis c_3 of the $FeBO_3$ crystals

$$f(Fe^{2+}, T) = \pm|C|\{(z'_1/z'_0)^2/[TB_{5/2}(x)]\} \quad (9)$$

in units of $|C|$ emu/g, where $|C|$ is the constant. It can be seen from Eq. (9) and [6] that there are two variants of the temperature behavior of the contributions of Fe^{2+} and Fe^{3+} ions to the weak ferromagnetic moment along the c_3 axis. As follows from Fig. 3, at the competition between the Fe^{2+} and Fe^{3+} contributions [6] one of the variants can lead to the existence of a compensation point and the other, to the significant increase in $\sigma_z(T)$ at low temperatures.

Note that at present there exists a theoretical quantitative estimation of the single-ion contribution to the weak ferromagnetic moment along the c_3 axis $\sigma_z(Fe^{3+}) = m_zM$, which yields

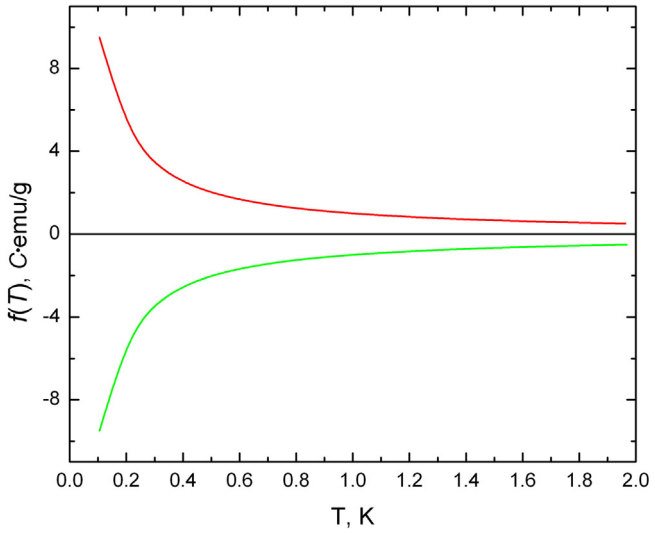

Fig. 3. Temperature dependence of $f(Fe^{2+},T)=\pm|C|\{(z_1'/z_0')^2/[TB_{5/2}(x)]\}$. The Brillouin function is taken to be unity due to the weak dependence in the investigated temperature range.

$2.4\cdot10^{-3} emu\cdot g^{-1}$ [6] at a temperature of T = 0 K. The experimental value is $\sigma_z(Fe^{3+},T=77K)=1.3\cdot10^{-3}\text{emu}\cdot g^{-1}$ [20,21]. In addition, note that in the $FeBO_3$ crystals with regard to the next-to-last term in Eq. (1) the point of compensation of the hexagonal anisotropy energy was experimentally observed at low temperatures [8].

5. Conclusions

As follows from Eq. (9) and Fig. 3, the maximum contribution at low temperatures will be given by the Fe^{2+} ions due to the strong $1/T$ dependence.

To explain more fully the temperature behavior of the weak ferromagnetic moment along the third-order axis of the $FeBO_3$ crystals, additional experimental investigations are needed. The discrepancy between the experimental and calculated values for the Fe^{3+} ions can be related, in particular, to different temperatures of their estimation and single-ion exchange contributions of Fe^{3+} ions [3,22].

Acknowledgment

The authors are grateful to E.V. Bondareva for paper translation and L.M. Rudenko for help with the paper layout.

Appendix A. Supplementary data

Supplementary data associated with this article can be found, in the online version, at https://doi.org/10.1016/j.jmmm.2018.01.037.

References

[1] V.E. Dmitrienko, E.N. Ovchinnikova, S.P. Collins, G. Nisbet, G. Beutier, Y.O. Kvashnin, V.V. Mazurenko, A.I. Lichtenstein, M.I. Katsnelson, Nat. Phys. 10 (2014) 202.
[2] A.M. Kalashnikova, A.V. Kumel, R.V. Pisarev, V.V. Gridnev, A. Kirilyuk, Th. Rasing, Phys. Rev. Lett. 99 (2007) 167205.
[3] S.G. Ovchinnikov, V.V. Rudenko, Uspekhi Fizicheskich Nauk 184 (2014) 1299.
[4] I.E. Dzyaloshinskii, Sov. Phys. JETP 5 (1957) 1259.
[5] E.A. Turov, Physical Properties of Magnetically Ordered Crystals, Izd. AN SSSR, Moscow, 1963.
[6] S.G. Ovchinnikov, V.V. Rudenko, V.I. Tugarinov, Phys. Solid State 58 (2016) 1995.
[7] M.H. Seavey, Sol. State Comm. 12 (1973) 49.
[8] V.D. Doroshev, I.M. Krygin, S.N. Lukin, A.N. Molchanov, A.D. Prokhorov, V.V. Rudenko, V.N. Seleznev, JETP Lett. 29 (1979) 257.
[9] S.G. Ovchinnikov, V.V. Rudenko, J. Cryst. Growth 455 (2016) 55.
[10] S.N. Lukin, V.V. Rudenko, V.N. Seleznev, G.A. Tsintsadze, Sov. Phys. Sol. State 22 (1980) 29.
[11] G.E. Barberis, R. Calvo, H.G. Maldonado, C.E. Zarate, Phys. B 12 (1975) 853.
[12] Yu. I. Sirotinin, M.P. Shaskol'skaya, Fundamentals of Crystal Physics, Nauka, Moscow, 1975.
[13] A. A. Abraham, B. Blini, Electron Paramagnetic Resonance of Transition Ions, Izdatelstvo Mir, M., (1972), vol. 1. p. 591.
[14] R.P. Hunt, J. Appl. Phys. 38 (1967) 2826.
[15] N.S. Piskunov, Differential and Integral Calculus, Nauka, Moscow, 1972.
[16] S. Krupichka, Physics of Ferrites and Related Magnetic Oxides, Mir, Moscow, 2, (1976), 50.
[17] A. Chlystov, S. Lukin, V. Rudenko, V. Seleznev, G. Tsintsadze, In Magnetic Resonance and Related Phenomena, in: Proc. of the XX Congress AMPERE, Tallin, August 21–26 1978, Springer, Berlin, 1979, p. 295.
[18] R.R. Sharma, T.P. Das, R. Orbach, Phys. Rev. 149 (1966) 257.
[19] S.A. Altshuler, B.M. Kozyrev, Electron Paramagnetic Resonance of Transition Group Element Compounds, Nauka, Mir, 1972.
[20] P.J. Flanders, J. Appl. Phys. 43 (1972) 2430.
[21] A.M. Kadomtseva, R.Z. Levitin, Yu.F. Popov, V.N. Seleznev, V.V. Uskov, Fizika Tverdogo Tela 14 (1972) 214.
[22] G.V. Bondarenko, S.G. Ovchinnikov, V.V. Rudenko, V.M. Sosnin, V.I. Tugarinov, A.M. Vorotynov, J. Magn. Magn. Mater. 335 (2013) 90.